RESEARCH ARTICLE | APRIL 18 2019

In situ observations for growth kinetics of water droplets on Bambusa multiplex leaves

Zhouyang Zhang; Linfeng Fei ; Dingjun Liu; Zhenggang Rao; Tingfang Tian; Yongming Hu ; Yu Wang

Appl. Phys. Lett. 114, 153702 (2019)
https://doi.org/10.1063/1.5090182

Applied Physics Letters ARTICLE scitation.org/journal/apl

In situ observations for growth kinetics of water droplets on Bambusa multiplex leaves

Cite as: Appl. Phys. Lett. **114**, 153702 (2019); doi: 10.1063/1.5090182
Submitted: 25 January 2019 · Accepted: 1 April 2019 ·
Published Online: 18 April 2019

View Online Export Citation CrossMark

Zhouyang Zhang,[1] Linfeng Fei,[2,a)] Dingjun Liu,[3] Zhenggang Rao,[1] Tingfang Tian,[1,b)] Yongming Hu,[4] and Yu Wang[1,c)]

AFFILIATIONS

[1]School of Materials Science and Engineering, Nanchang University, Jiangxi 330031, China
[2]Department of Applied Physics, The Hong Kong Polytechnic University, Hong Kong, China
[3]Institute of Advanced Sciences, Nanchang University, Jiangxi 330031, China
[4]Hubei Key Laboratory of Ferro- and Piezoelectric Materials and Devices, Faculty of Physics & Electronic Science, Hubei University, Wuhan 430062, China

[a)]Electronic mail: feilinfeng@gmail.com
[b)]Electronic mail: tftian@ncu.edu.cn
[c)]Electronic mail: wangyu@ncu.edu.cn

ABSTRACT

The wetting of material surfaces is an important topic and is now being intensively investigated toward various practical applications, yet most previous studies have adopted postmortem methods. Fortunately, the recent development of environmental scanning electron microscopy (ESEM) means that hydrated samples can be observed in their native state, as well as dynamic surface reactions. Here, we use *in situ* ESEM observation to explore the microscopic growth dynamics of water droplets on adaxial and abaxial surfaces of Bambusa multiplex leaf (BML) during wetting. Our results show that, due to the dramatic structural differences between adaxial and abaxial surfaces, the growth of water droplets on the two sides is quite different. Furthermore, the growth kinetics of water droplets on different BML surfaces are quantitatively discussed. This conceptual study demonstrates a straightforward pathway to understanding the wetting behavior, and the results may pave the way for further research on bio-inspired materials.

Wetting is a process where the gas surrounding a solid surface is replaced by direct liquid contact. As a common liquid-solid interaction, wetting is a classic topic in physical chemistry and is significant in various applications such as microfluid devices, surface treatment, and biomimetic material design.[1–5] For example, the wetting behavior on biological surfaces is intimately related to their microstructural features; according to Jiang *et al.*, special micro- and nanostructures on the surfaces of lotus leaves play a determinative role in their superhydrophobic properties.[6] In recent years, increasing attention has been paid to the relationship between the surface morphology/structure and wettability in materials science.[7,8] Earlier results suggest that many biological material surfaces exhibit superhydrophobic properties; these include lotus leaves,[9] rice leaves,[10] water bamboo leaves,[11] water strider legs,[12] and mosquito compound eyes.[13]

Conventional methods for characterizing the wetting of material surfaces rely on postmortem examination of the surfaces, using scanning electron microscopy (SEM) or contact angle (CA) tests with optical microscopy.[14] For example, Guan *et al.* used these postmortem examinations and theoretical analysis on water bamboo leaves to investigate the impact of structures on wettability,[11] and Lai *et al.* designed three different types of superhydrophobic nanostructures that were characterized using SEM and water CA.[15] However, we consider that the recent development of environmental scanning electron microscopy (ESEM)[16–19] provides us with an unparalleled opportunity to directly observe the microstructures and microscopic reactions in a quasi-natural environment, including the wetting of solid surfaces and the evolution of water droplets during condensation or evaporation.[20–23] Additionally, *in situ* observations based on ESEM can provide clear kinetic information during the whole process, which is not accessible by *ex situ* experimental probes, and reveal further insight into the effects of the structure on wettability.

Bambusa multiplex leaves (BMLs), from southern China, represent a typical system with naturally different wettabilities on adaxial and abaxial surfaces and can be an appropriate choice for investigating

the relationship between the structure and wettability. Moreover, microscopic studies of material surfaces, together with direct observations of water-surface interactions, are crucial to the design and manufacture of functional biomimetic materials.[24–27] Inspired by our previous *in situ* studies of crystal growth,[28–32] particularly the study of ice growth in ESEM,[33] we use here an advanced ESEM setup to implement *in situ* observations of the microscopic structure-induced growth dynamics of water droplets during condensation on adaxial and abaxial surfaces of BML. We reveal the microstructural differences between adaxial and abaxial BML surfaces, as well as the distinct wetting dynamics on both surfaces. Consequently, the wetting behavior on both sides of BML is quantitatively analyzed, in terms of contact angles and sizes of water droplets as a function of time. The results should lead to a better understanding of wetting processes in nature, and the technique developed in this work could be extended more generally to research on other interfacial processes.

We first measured the contact angles of water on adaxial and abaxial surfaces of BML (Fig. S1) to determine the surface wettability. The adaxial surface has a water CA of $71.3 \pm 0.58°$, which is hydrophilic according to classic Young's theory. On the other hand, the CA of the abaxial surface was $133.9 \pm 1.27°$. This value is smaller than that previously reported by Guan, for the superhydrophobic surface of water bamboo (CA of $\sim 151°$),[11] indicating different surface structures. Fresh BMLs were then transferred into the specimen chamber of ESEM on a cooling stage, after thorough and careful cleaning. The experiment was carried out under strictly controlled environmental parameters throughout the observation (temperature, $-3\,^{\circ}C$; pressure, 500 Pa; and relative humidity, 100%). Figure 1 shows ESEM micrographs for both surfaces of the BML. As can be seen, the adaxial surface is basically smooth [Fig. 1(a)], with only a few prickles [an example of which is denoted as 1 in Fig. 1(b)] and shallow grooves, while the abaxial surface is more complex. As shown in Figs. 1(d) and 1(e), the abaxial surface is completely covered by patterned grooves, some stomata [e.g., denoted as 2 in Fig. 1(d)], many papillae [e.g., denoted as 3 in Fig. 1(e)], and a few prickles [e.g., denoted as 4 in Fig. 1(e)]. The papillae, of about 8 μm in height and 5 μm in diameter, are arranged with an average separation distance of 12 μm. The papillae, as well as the root of the abaxial prickles [Fig. 1(e)], are surrounded by various disordered nanostructures. In comparison to previous results for a lotus leaf,[34] the average length of branch-like nanostructures for a single papilla of a BML is about 700 nm; the surface nanostructures here occur with a much lower density and larger sizes as shown in Fig. 1(f).

We performed further *in situ* experiments with ESEM to observe the growth of water droplets on BML surfaces. Due to the topographical differences between the two sides of the BML, we carried out experiments on the adaxial and abaxial surfaces separately. Figures 2(a)–2(c) show representative frames for water droplet growth on the adaxial surface. As shown in Fig. 2(a), at the initial stage, water droplets nucleate preferentially at surface concavities (grooves, creases, and tip of prickles), which are preferred for heterogeneous nucleation because of their roughness. Then, as the water molecules (or small water droplets) continue to be absorbed into the nucleus, small droplets further develop themselves on the surface. Finally, when two (or more) droplets come into contact with each other upon further growth [Fig. 2(c)], they coalesce to form a large droplet under the Laplace pressure, so that the larger droplet absorbs the smaller ones [as shown

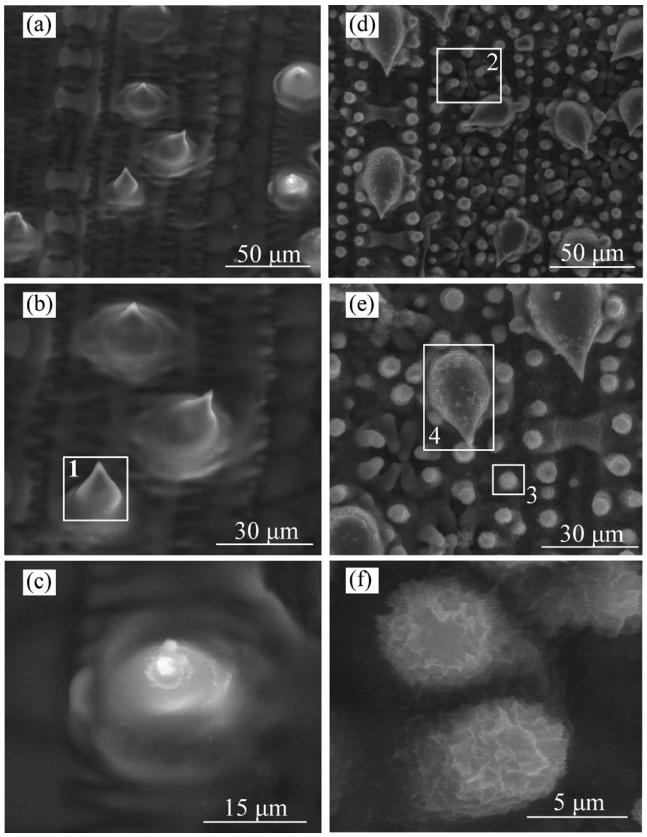

FIG. 1. ESEM images of adaxial and abaxial BML surfaces; (a)–(c) adaxial surface; and (d)–(f) abaxial surface. Arabic numerals 1 and 4 denote prickles, 2 denotes a stoma surrounded by seven or eight papillae, and 3 denotes a papilla. (c) Magnified image of a prickle on the adaxial surface. (f) Magnified image of a papilla on the abaxial surface.

in white rectangles in Figs. 2(a)–2(c)]. In this process, for the droplets on the base-layer, the supply of water from the gas phase is stable (vapor pressure and humidity are maintained as constants, and adsorption energy for water droplets is small due to the smooth surface); therefore, the droplet size evolves steadily on this surface. On the other hand, on the tips of prickles (refer to yellow squares in Fig. 2), further growth of these droplets was significantly depressed [Figs. 2(b) and 2(c)], even though we noted that the nucleation of water occurred synchronously with that on the base-layer [Fig. 2(a)]. We believe that, due to the conical shape of the prickles [Fig. 1(e)], the droplets tend to generate near the base of the prickle, since the Laplace pressure on the high-curvature tip is larger than that on the low-curvature base, because the radius of the tip is smaller than the radius of the base.

Similarly, the water condensation dynamics on the abaxial surface was also recorded, as summarized in Figs. 2(d)–2(f). At the initial stage [Fig. 2(d)], tiny water droplets preferentially nucleate on top of prickles (yellow squares) and areas between papillae (white rectangles), including the stomata, which are surrounded by seven or eight papillae, and behave as concavities. Subsequently [Fig. 2(e)], the growth of droplets is delimited by the papillae, so that the droplets develop with

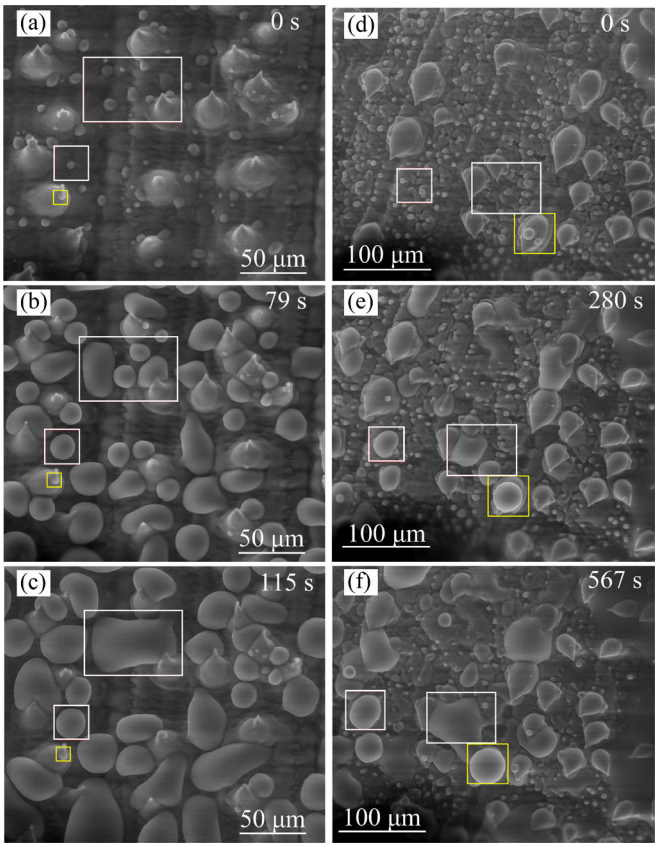

FIG. 2. ESEM image series of growth of water droplets on the BML surfaces. (a)–(c) Droplet growth on the adaxial surface at (a) 0 s, (b) 79 s, and (c) 115 s. The white rectangles indicate growth dynamics on the base-layer, while the yellow squares indicate the process on a prickle. (d)–(f) Droplet growth on the abaxial surface at (d) 0 s, (e) 280 s, and (f) 567 s. The white rectangles indicate growth dynamics on stomata (spacing areas) of papillae, while the yellow squares indicate the process at the top of a prickle.

roughly stable CAs, and this delimiting is a similar phenomenon to that previously reported for lotus leaves.[35] Thereafter [Fig. 2(f)], two or more neighboring droplets can merge into continuous water membranes when they meet each other. Notably, water droplets on the tips of prickles also grow with time in this case [refer to yellow squares in Figs. 2(d)–2(f)]. Compared to the growth on prickles, it is much easier for droplets to develop on papillae-layers because the CA is much smaller. We believe that the capillary condensation effect, which is caused by the existence of abundant three-dimensional nanostructures (the papillae), accelerates the nucleation and growth of water films. The capillary condensation occurs due to the roughness on the abaxial surface, so that many tiny droplets form together on the surface, especially at defects, and their later growth depends on transportation of water from the gaseous phase. In addition, an adhesion effect, caused by the rough papillae and tops of prickles, leads to a higher contact angle on the abaxial surface. In our experiment, the water vapor was at a supersaturated level throughout the condensation process. According to classical nucleation theory,[20] because of the larger CA of prickles than that of papillae-layers, the free energy barrier for prickles is larger than that for papillae-layers, while the critical radius is the same; as a result, water droplets need more energy to nucleate on prickles. Therefore, nucleation and growth of water droplets occur much more readily on the papillae-layers.

To obtain a better understanding of the wetting behavior, the diameters of water drops on different parts of a BML were measured with respect to time and are shown in Fig. 3. The relationship between the diameter of the droplet (r) and its growing time (t), during condensation, can be described by the following relation:[36]

$$r \propto t^{\alpha},$$

where α is the power law exponent, which ranges from 0 to 1. During the growth of a droplet, the exponent (α) can be influenced by factors such as gas flow, substrate conditions (temperature, topography, and wettability), and geometry of the droplet. Figure 3(a) shows quantitatively the growth dynamics of droplets on different BML surfaces (the

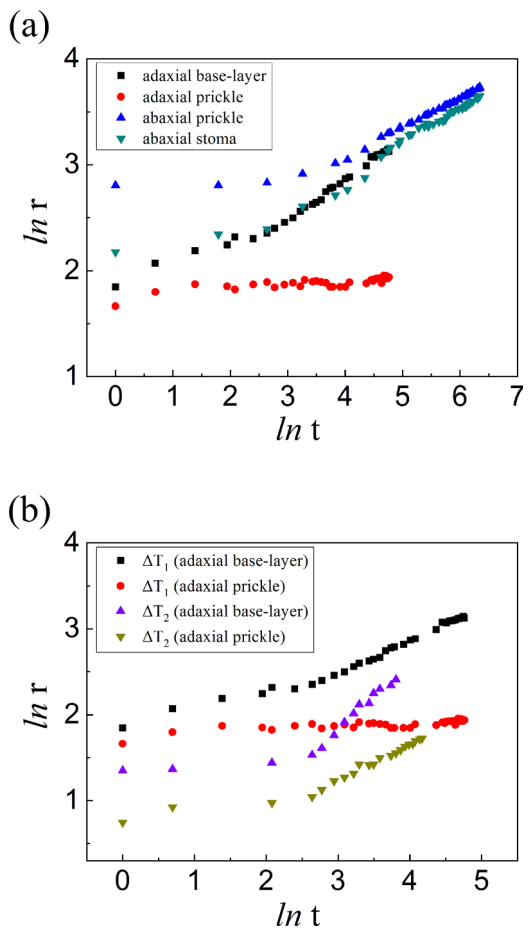

FIG. 3. Statistical distribution of the time-dependent droplet size during our observation; the data sources are shown in the supplementary material as Figs. S2–S4. (a) Droplet size as a function of time for different parts of the BML surface at ΔT_1, (b) Relationship for adaxial parts at different ΔT ($\Delta T_1 = -1.1\,^{\circ}C$ and $\Delta T_2 = -2.2\,^{\circ}C$). The units of r and t are micrometer and second, respectively.

corresponding images are given in Figs. S2 and S3). Growth of water droplets on the adaxial base-layer (black squares), abaxial stoma (green triangles), and abaxial prickle (blue triangles) could be divided into two distinct stages. In the first stage, droplets grew slowly and α was determined to be smaller than 0.2. Specifically, α on the base-layer, stoma, and abaxial prickle was calculated to be 0.18, 0.12, and 0.06, respectively. For the abaxial surface, the α value for the stoma is slightly higher; this may result from the additional capillary forces contributed by the surrounding papillae. In contrast, α is smaller for the abaxial surface prickle due to its spherical geometry. During this stage, the determining growth factor should be surface migration of water, because the small droplet with small surface area cannot efficiently absorb water from the gas phase. In the second stage, the droplets grew faster. The exponents (α) on the base-layer, stoma, and prickle were 0.39, 0.35, and 0.26, respectively, and the dominant water source of droplet growth should be water vapor, considering the surrounding droplets on the leaf surface have been consumed during surface migration on the initial stage. These results show that the major source of water for droplet growth changes from surface migration (initial stage) to gas-phase transportation (later stage). However, the droplets on the tips of adaxial prickles (red circles) grew slowly, with an α value of only 0.04. Note that the material of adaxial and abaxial surfaces can be treated as the same for our observation areas; therefore, the distinct growth behaviors on two sides should be attributed to the structural differences, as revealed in Fig. 1.

We also found that a temperature decrease can actually accelerate the droplet growth. We defined $\Delta T = T - T_{g,l}$ ($T_{g,l}$ is the gas-liquid equilibrium temperature of water under 500 Pa, approximately equal to $-2.8\,^{\circ}C$ according to the phase diagram for water). Two sequences of images are shown in Figs. S3 and S4, of droplet growth on the adaxial surface, captured under the same pressure (500 Pa) but different temperatures, $-3.9\,^{\circ}C$ and $-5\,^{\circ}C$, respectively. These are summarized in Fig. 3(b), with $\Delta T_1 \approx -1.1\,^{\circ}C$ for the base-layer (black squares) and prickles (red circles) and $\Delta T_2 \approx -2.2\,^{\circ}C$ for the base-layer (purple triangles) and prickles (dark yellow triangles), on the adaxial surface, showing different growth behaviors for different ΔT ($-1.1\,^{\circ}C$ and $-2.2\,^{\circ}C$). The change of ΔT shows little influence on growth during the first stage, but the growth rates are dramatically increased for the lower temperature, during the second stage. It can be seen that α for the base-layer and prickles reached 0.77 and 0.42, respectively, when the temperature was reduced by $1.1\,^{\circ}C$. With the help of photos taken using the ESEM, we found that the nucleation density also rapidly increased with the increase in ΔT, on every part of the surface. Moreover, the droplets grow and merge with each other more quickly at lower under-cooling temperatures.

In summary, we have demonstrated the *in situ* ESEM experiments concerning the dynamics of surface-structure-dependent water droplet growth on BML surfaces. Adaxial and abaxial BML surfaces have been revealed to possess different microscale structures, causing different wetting processes during water condensation. Furthermore, we have microscopically identified and quantitatively compared the interesting growth dynamics of different parts of both surfaces, which show major changes in the water source, from surface migration to gas-phase transportation, during the condensation process. Our study, using an *in situ* ESEM technique, provides an effective method for investigating dynamic processes in biorelated materials and could be useful in guiding the design of bio-inspired materials.

See supplementary material for Fig. S1, photos of BML and water contact test on BML surfaces; Fig. S2, ESEM image series of growth of water droplets on the abaxial surface with ΔT of about $-1.1\,^{\circ}C$; Fig. S3, ESEM image series of growth of water droplets on the adaxial surface with ΔT of about $-1.1\,^{\circ}C$; Fig. S4, ESEM image series of growth of water droplets on the adaxial surface with ΔT of about $-2.2\,^{\circ}C$.

The authors acknowledge the support from the National Science Foundation of China (Project Nos. 51562026, 11574126, and 51702149) and Jiangxi's Natural Science Foundation (Project Nos. 20171ACB20006 and 20171BAB216011). Z.Z. acknowledges the support from Jiangxi's Creative Project for Graduate Students (Project No. YC2017-S004). Y.H. acknowledges the support from Special Funds for Public Science and Technology Innovation Platform Construction in Hubei Province (Project No. 2018BEC483).

REFERENCES

[1]X. J. Feng and L. Jiang, Adv. Mater. **18**, 3063 (2006).
[2]B. Bera, O. Carrier, E. H. G. Backus, M. Bonn, N. Shahidzadeh, and D. Bonn, Langmuir **34**, 12344 (2018).
[3]M. Tuominen, H. Teisala, J. Haapanen, J. M. Makela, M. Honkanen, M. Vippola, S. Bardage, M. E. P. Walinder, and A. Swerin, Appl. Surf. Sci. **389**, 135 (2016).
[4]C. Yuan, M. Y. Huang, X. J. Yu, Y. P. Ma, and X. B. Luo, Appl. Surf. Sci. **385**, 562 (2016).
[5]X. Chen, J. N. Chen, X. L. Ouyang, Y. Song, R. N. Xu, and P. X. Jiang, Langmuir **33**, 6701 (2017).
[6]X. Yao, Y. L. Song, and L. Jiang, Adv. Mater. **23**, 719 (2011).
[7]A. Giacomello, L. Schimmele, S. Dietrich, and M. Tasinkevych, Soft Matter **12**, 8927 (2016).
[8]A. Yagub, H. Farhat, S. Kondaraju, and T. Singh, J. Comput. Phys. **301**, 402 (2015).
[9]K. S. Liu, X. Yao, and L. Jiang, Chem. Soc. Rev. **39**, 3240 (2010).
[10]D. Wu, J. N. Wang, S. Z. Wu, Q. D. Chen, S. A. Zhao, H. Zhang, H. B. Sun, and L. Jiang, Adv. Funct. Mater. **21**, 2927 (2011).
[11]H. Y. Guan, Z. W. Han, H. N. Cao, S. C. Niu, Z. H. Qian, J. F. Ye, and L. Q. Ren, J. Bionic Eng. **12**, 624 (2015).
[12]X. F. Gao and L. Jiang, Nature **432**, 36 (2004).
[13]X. F. Gao, X. Yan, X. Yao, L. Xu, K. Zhang, J. H. Zhang, B. Yang, and L. Jiang, Adv. Mater. **19**, 2213 (2007).
[14]M. He, J. J. Wang, H. L. Li, and Y. L. Song, Soft Matter **7**, 3993 (2011).
[15]Y. K. Lai, X. F. Gao, H. F. Zhuang, J. Y. Huang, C. J. Lin, and L. Jiang, Adv. Mater. **21**, 3799 (2009).
[16]J. Ha, J. Kim, Y. Jung, G. Yun, D. N. Kim, and H. Y. Kim, Sci. Adv. **4**, eaao7051 (2018).
[17]H. J. Cho, D. J. Preston, Y. Y. Zhu, and E. N. Wang, Nat. Rev. Mater. **2**, 16092 (2017).
[18]K. Rykaczewski, J. H. J. Scott, and A. G. Fedorov, Appl. Phys. Lett. **98**, 093106 (2011).
[19]B. Carrier, L. L. Wang, M. Vandamme, R. J. M. Pellenq, M. Bornert, A. Tanguy, and H. Van Damme, Langmuir **29**, 12823 (2013).
[20]K. K. Varanasi, T. Deng, J. D. Smith, M. Hsu, and N. Bhate, Appl. Phys. Lett. **97**, 234102 (2010).
[21]M. Nosonovsky and B. Bhushan, Nano Lett. **7**, 2633 (2007).
[22]B. Bhushan and Y. C. Jung, J. Phys.-Condens. Matter **20**, 225010 (2008).
[23]K. Koch, B. Bhushan, and W. Barthlott, Soft Matter **4**, 1943 (2008).
[24]A. Ashrafi and A. Moosavi, J. Appl. Phys. **120**, 124901 (2016).

[25]H. Cha, C. Y. Xu, J. Sotelo, J. M. Chun, Y. Yokoyama, R. Enright, and N. Miljkovic, Phys. Rev. Fluids **1**, 064102 (2016).
[26]Y. M. Hou, M. Yu, X. M. Chen, Z. K. Wang, and S. H. Yao, ACS Nano **9**, 71 (2015).
[27]Y. M. Zheng, D. Han, J. Zhai, and L. Jiang, Appl. Phys. Lett. **92**, 084106 (2008).
[28]L. F. Fei, T. Y. Sun, W. Lu, X. Q. An, Z. F. Hu, J. C. Yu, R. K. Zheng, X. M. Li, H. L. W. Chan, and Y. Wang, Chem. Commun. **50**, 826 (2014).
[29]L. F. Fei, S. M. Ng, W. Lu, M. Xu, L. L. Shu, W. B. Zhang, Z. H. Yong, T. Y. Sun, C. H. Lam, C. W. Leung, C. L. Mak, and Y. Wang, Nano Lett. **16**, 7875 (2016).
[30]L. F. Fei, W. Lu, Y. M. Hu, G. Y. Gao, Z. H. Yong, T. Y. Sun, N. G. Zhou, H. S. Gu, and Y. Wang, J. Mater. Chem. A **5**, 3786 (2017).
[31]L. F. Fei, S. J. Lei, W. B. Zhang, W. Lu, Z. Y. Lin, C. H. Lam, Y. Chai, and Y. Wang, Nat. Commun. **7**, 12206 (2016).
[32]L. F. Fei, X. L. Gan, S. M. Ng, H. Wan, M. Xu, W. Lu, Y. C. Zhou, C. W. Leung, C. L. Mak, and Y. Wang, ACS Nano **13**, 681 (2019).
[33]Z. Y. Zhang, L. F. Fei, Z. G. Rao, D. J. Liu, C. W. Leung, and Y. Wang, Cryst. Growth Des. **18**, 6602 (2018).
[34]L. Feng, S. H. Li, Y. S. Li, H. J. Li, L. J. Zhang, J. Zhai, Y. L. Song, B. Q. Liu, L. Jiang, and D. B. Zhu, Adv. Mater. **14**, 1857 (2002).
[35]Y. T. Cheng, D. E. Rodak, A. Angelopoulos, and T. Gacek, Appl. Phys. Lett. **87**, 194112 (2005).
[36]N. Miljkovic, R. Enright, and E. N. Wang, ACS Nano **6**, 1776 (2012).